MODELING SURFACE AND SUBSURFACE RUNOFF IN A FORESTED WATERSHED

By David H. Axworthy,[1] Associate Member, ASCE, and Bryan W. Karney,[2] Member, ASCE

ABSTRACT: A hydrologic model, capable of approximating surface and subsurface runoff from a forested shallow-soil watershed without the time of concentration parameter, is developed. A watershed is modeled as a series of vertically and horizontally linked nonlinear storages, each represented by a lumped mass-balance equation. The resulting system of ordinary differential equations is evaluated by the fourth-order Runge-Kutta finite-difference method. Comparison of this simpler modeling approach with method of characteristics and Petrov-Galerkin finite-element solutions shows good agreement. However, because the performance of the preliminary formulation on a forested watershed was unsatisfactory, an extended subsurface model is developed that explicitly accounts for the presence of both the soil and the small channels between the soil layer and bedrock face. Application of the extended model to the same forested watershed shows significantly improved agreement between the observed and computed runoff hydrographs.

INTRODUCTION

The primary goal of hydrologic modeling is to represent the response of a flow system to spatially and temporally changing inputs and conditions. Although it is difficult to gain a detailed understanding of individual hydrologic processes, it is possible to model the natural system by replacing it with a simplified yet similar structure (Singh 1988). This simplified structure is typically a collection of subsystems each representing individual hydrologic processes. Based on physical relationships, hydrologic processes are modeled as sets of equations, such as nonlinear partial differential equations, to describe the relationships between the processes and their corresponding variables. The solution of these equation sets is seldom trivial, prompting the development of many complex techniques to meet the challenge.

The belief that predictive accuracy is proportional to model complexity has led to the proliferation of complex two-dimensional finite-difference (e.g., James and Kim 1990) and finite-element-based models (e.g., Julien and Moglen 1990; Muñoz-Carpena et al. 1993) that require vast amounts of hydrologic data and that, over time, have acquired a reputation as some of the most highly accurate simulation techniques available. However, modeling assumptions inherent within a complex simulation are often just as limiting as those used in the development of simple techniques (Sloan and Moore 1984). In fact, Sloan and Moore (1984) suggest that numerical modelers can achieve good predictive accuracy modeling subsurface flow with a simple storage model without resorting to complex two-dimensional finite-element techniques. Therefore, it seems more efficient, both in terms of computational run time and the cost of data acquisition, to also pursue the development of simpler models.

The application and utility of simple hydrologic modeling techniques are demonstrated here using a forested shallow-soil watershed. Dissolved organic carbon (DOC) analysis of infiltrated water at various soil depths in a forested watershed by Jardine et al. (1989, 1990) showed that preferential vertical flow pathways exist in the soil cover. Later, Peters et al. (1995) found that a significant fraction of event water falling on forested shallow-soil hillslopes rapidly infiltrates to the impermeable bedrock, where it is readily transported downslope across the bedrock face. Further DOC analysis by Peters et al. (1995) showed that the remaining fraction of event water is transported downslope via Darcian matrix flow with a portion being stored in the hillslope as it mixes with or displaces preevent water. It is the contention of this paper that the forested shallow-soil watershed surface and subsurface storage processes described above, can be satisfactorily approximated by a simple storage model without resorting to more complex modeling techniques.

MODELING APPROACH

Watershed runoff is modeled as a series of linked nonlinear storages, herein referred to as *subcatchments*. In effect, this is a discrete representation of a continuous process. Each subcatchment is an independent, quasi-steady storage element mathematically represented by lumped continuity and momentum relations. More specifically, a subcatchment is a tiered system of planes in which overland or surface flow is modeled on the upper plane and ground-water or subsurface flow is modeled on the lower plane. Each subcatchment represents a physically identifiable finite area of the hydrologic basin and can be independently defined in terms of physical dimensions, infiltration capacity, surface and subsurface slope, hydraulic resistance, and saturated hydraulic conductivity. The transport processes in each subcatchment are approximated by existing formulas (e.g., Manning's equation, Green-Ampt method, Darcy's Law), and subcatchments are linked to each other via overland and ground-water flow. Computed surface and subsurface discharges on the final subcatchment represent the contribution from the entire catchment. As is discussed in detail later, the Runge-Kutta method is used to sequentially evaluate each ordinary differential equation representing the spatially lumped mass-balance equations for both the surface and subsurface planes of each subcatchment.

SURFACE STORAGE

Using a finite-volume formulation, the mass-balance equation representing the rate of change f_s of total surface water depth for the subcatchment can be written as

$$f_s[t, D(t)]_j = \frac{d(D_p + D_t)_j}{dt} = aP + q_{j-1} - q_j - f_i - E \quad (1)$$

where $D = (D_p + D_t)_j$ = total surface storage depth on subcatchment j; t = time; D_p = depression storage depth; D_t = detention storage depth; P = base rate of rainfall; a = adjust-

[1]Res. Assoc., Dept. of Civ. Engrg., Univ. of Toronto, Toronto, Canada, M5S 1A4.
[2]Prof., Dept. of Civ. Engrg., Univ. of Toronto, Toronto, Canada.

Note. Discussion open until September 1, 1999. To extend the closing date one month, a written request must be filed with the ASCE Manager of Journals. The manuscript for this paper was submitted for review and possible publication on April 25, 1996. This paper is part of the ***Journal of Hydrologic Engineering***, Vol. 4, No. 2, April, 1999. ©ASCE, ISSN 1084-0699/99/0002-0165–0173/$8.00 + $.50 per page. Paper No. 13145.

able scale factor used to account for factors such as return period and interception storage; q_{j-1} = overland flow from subcatchment $j-1$ that is directly upstream of subcatchment j; q_j = overland flow from subcatchment j; f_i = infiltration rate; and E = evapotranspiration rate. For laminar overland flow, surface runoff is

$$q = \frac{\mathbf{g} S D_t^3}{3\nu L_c} \tag{2}$$

where $\mathbf{g}$ = acceleration due to gravity; S = slope of subcatchment surface; ν = kinematic viscosity; and L_c = representative dimension of subcatchment parallel to direction of flow. Delineation of the transition from laminar to turbulent flow is left to the discretion of the analyst. However, Chow et al. (1988, p. 37) suggest that, for a smooth-surfaced channel of infinite width, this transition occurs at a Reynolds number of 2000, with values beyond this threshold indicating that overland flow is turbulent. To determine the rate of turbulent overland flow, Manning's equation is convenient

$$q = \frac{C_u}{nL_c} D_t^{5/3} S^{1/2} \tag{3}$$

in which C_u = constant depending on units, and n = Manning's roughness coefficient. In (3), the hydraulic radius is approximated by the detention storage depth because the ratio of the subcatchment width W_c (i.e., dimension of subcatchment perpendicular to direction of flow) to the detention storage depth (i.e., W_c/D_t) is large (i.e., greater than 10). A variety of infiltration models, such as Horton (1933), Holtan (1961), and Green and Ampt (1911) can be selected. Once the subsurface storage is filled, water is exfiltrated at the same rate and opposite sign as the computed infiltration rate. Infiltration capacity is regenerated during a rainfall hiatus. Evapotranspiration from both surface depression and detention storage is computed by the methods of Priestley and Taylor (1972), although alternate methods can easily be employed if appropriate data is available.

SUBSURFACE STORAGE

Again using a finite-volume formulation, the mass-balance equation governing the rate of change of subsurface water depth f_g for the subcatchment can be written as

$$f_g[t, H(t)]_j = \frac{d(H_r + H_d)_j}{dt} = \frac{f_i + g_{j-1} - g_j - E}{\varepsilon} \tag{4}$$

where ε = soil porosity and accounts for porous medium storage; $H = (H_r + H_d)_j$ = total subsurface storage depth in subcatchment j; H_d = drainable depth of water stored in hillslope saturated zone; H_r = retention storage; g_{j-1} = subsurface runoff from subcatchment $j-1$ directly upstream of subcatchment j; and g_j = subsurface runoff from subcatchment j. Subsurface runoff is calculated by Darcy's Law

$$g = K_h \frac{H_d}{L_c} \frac{dH_d}{dx} \tag{5}$$

where K_h = horizontal saturated hydraulic conductivity and dH_d/dx = hydraulic gradient. The subsurface dimensions (i.e., length and width) are identical to the surface dimensions of the subcatchment, and dH_d/dx is approximated by the slope of the subsurface bed S_g (see Beven 1981; Engman and Rogowski 1974). Retention storage depth H_r is measured as a percentage of the equivalent depth of subsurface water content ω. This is, $H_r = \omega_r(\omega H_d)$ where ω_r = fraction of the total porous media storage available for storage of retained water. Retention storage is only depleted by evapotranspiration.

Surface-Subsurface Linkage

The surface and subsurface mass balance equations are linked vertically, since infiltration is both an outflow from the surface and an inflow to the subsurface. In forested shallow-soil watersheds, the vertical hydraulic conductivity of the soil is often high, resulting in rapid conduction of infiltrated water from the near surface of the subcatchment through the soil matrix to the subsurface boundary below. Although this type of linkage may limit the applicability of this modeling approach to shallow-soil watersheds, more research is required to confirm this statement. In fact, the release of subsurface runoff in the soil matrix may also play a significant role in the surface-subsurface linkage. For example, a low subsurface release rate may cause exfiltration on the surface of the subcatchment if the soil matrix becomes saturated. In this case, the surface-subsurface linkage process is effectively reversed.

NUMERICAL APPROACH

The surface-subsurface mass-balance equation pair can sometimes be solved analytically by the method of characteristics (MOC). Although the MOC is a useful tool for analyzing simple catchments, it is difficult to implement in complex watersheds. Many popular engineering hydrologic numerical models (e.g., SWMM and STORM) essentially utilize the Euler method (e.g., Huggins and Monke 1968). However, this too is often impractical for hydrologic modeling because it is prone to numerical error when the spatial step size is large, and instability may develop when it is small. For example, Fig. 1 illustrates the development of instabilities on a 500-m-long catchment with a spatial step size of 13.158 m. Reducing the time step increases both the stability of the Euler technique, and the execution time.

An alternative to reducing the time step is to use an explicit finite-difference technique of higher order, such as the ''classic'' fourth-order Runge-Kutta method. Flanagan and Livingston (1995) used the Runge-Kutta method to solve the surface storage problem. To propagate the solution, the Runge-Kutta method generates an average propagation rate from the weighted average of four evaluations of the differential equation. These include evaluations at the beginning, at the midpoint, and at the end of the time interval. For example, the total surface storage depth at any time t is approximated by the method as

$$D(t + \Delta t) = D(t) + \frac{1}{6}(k_1 + 2k_2 + 2k_3 + k_4) + O(\Delta t^5) \tag{6}$$

in which

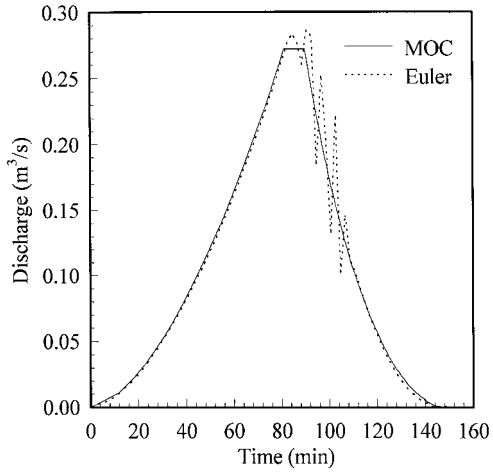

FIG. 1. Eulerian Finite-Difference Solution Instability

J. Hydrol. Eng. 1999.4:165-173.

$$k_1 = \Delta t \cdot f_s[t, D(t)], \quad (7)$$

$$k_2 = \Delta t \cdot f_s[t + \Delta t/2, D(t) + k_1/2], \quad (8)$$

$$k_3 = \Delta t \cdot f_s[t + \Delta t/2, D(t) + k_2/2], \text{ and} \quad (9)$$

$$k_4 = \Delta t \cdot f_s[t + \Delta t, D(t) + k_3] \quad (10)$$

In the same manner, the total subsurface storage depth is computed simultaneously. A better average propagation rate permits the use of larger time increments than is possible with a Eulerian solution, thus achieving a higher degree of accuracy and greater stability with little computational expense. Although this modeling approach is fourth-order in time, it is only first-order in space. Before comparing the Runge-Kutta approach to existing models, it is instructive to study the model's sensitivity to both spatial and temporal grid step size.

MODEL SENSITIVITY TO SPATIAL AND TEMPORAL STEP SIZE

Since the Runge-Kutta representation used here is explicit, the Courant condition must be satisfied to guard against instability when the spatial (Δx) and temporal (Δt) step sizes are varied. Although the Courant condition does not guarantee stability, it does ensure that an adequate number of points in the spatial and temporal grid are available to numerically propagate the equation pairs within the limits of the kinematic wavespeed (Press et al. 1988). The largest kinematic wavespeeds occur during the maximum depth of surface-subsurface flow; therefore, a conservative test for stability is obtained from the Courant condition by using the peak depth of overland flow y_{pk} in the wavespeed calculation. If Manning's equation is differentiated with respect to the depth of overland flow, the Courant condition is

$$C_r = \frac{\left| \frac{5}{3n} C_u y_{pk}^{2/3} S^{1/2} \right| \Delta t}{\Delta x} \leq 1 \quad (11)$$

in which C_r = Courant number. For illustrative purposes, the sensitivity analysis is demonstrated with surface flow; however, the conclusions are equally applicable to subsurface flow.

Test Catchment

A simple 100 × 500 m hypothetical plane is chosen with parameters typical of a sandy clay loam underlying a grassy floodplain. The catchment has an average slope of 2%, a Manning's roughness coefficient of 0.035, and a constant infiltration capacity of 5.26 mm/h. In addition, a precipitation rate of 15 mm/h is assumed uniform and constant throughout the 60-minute storm duration t_r. Numerical results are compared with an MOC analytical solution to assess the sensitivity of the modeling approach under varying spatial and temporal conditions. For this test, the MOC analytical solution determines the maximum depth of overland flow y_{pk} to be 8.12 mm and the corresponding maximum unit discharge $q_{L,max}$ to be 1.324×10^{-3} m^2/s. In the next section, numerical results from the sensitivity analysis are presented in nondimensional form by dividing maximum values by those from the MOC analytical solution.

Sensitivity Analysis

The purpose of this study is to determine the minimum number of computational steps required to achieve a desired numerical accuracy without developing numerical instabilities. Since more than one series is required, a discrete number of spatial steps N_{space} are chosen. This sufficiently describes the behavior of the modeling approach under variable conditions while limiting the number of trials undertaken. The number of spatial steps represents the number of subcatchments used to model the test catchment. Discretization of the temporal and spatial grid is not referenced in absolute terms, as the results of a sensitivity analysis are intended to be independent of catchment dimension or time frame. N_{time} is selected to represent the number of time steps equivalent to the storm duration.

Computational efficiency is a relative term, as much a function of the desired accuracy as of the CPU time required to achieve this accuracy. As Fig. 2 illustrates, the higher the Courant number, the fewer the number of computational steps required to achieve a specified accuracy. In addition, Fig. 2 shows that computational effort rapidly increases with a decreasing Courant number. For example, a simulation with $C_r \leq 1.0$ required 780 computational steps (spatial grid spacing × temporal grid spacing) to achieve an accurate peak flow, while a simulation with $C_r \leq 0.4$ required 1,960 computational steps to achieve the same level of accuracy. Further details are found in Axworthy (1993).

In Fig. 3, the fourth-order Runge-Kutta finite-difference solution of the storage equation pairs is presented for a number of spatial and temporal grid spacing trials. The number of spatial and temporal steps for each trial are given as (N_{space}, N_{time}) pairs as follows: A = (2, 4); B = (3, 6); C = (5, 10); D = (10, 19); E = (20, 39); and F = (40, 79). A maximum Courant number of 1.0 is maintained for each trial. The overland flow q_L is nondimensionalized by dividing by the maximum discharge $q_{L,max}$ as computed from the MOC analytical solution

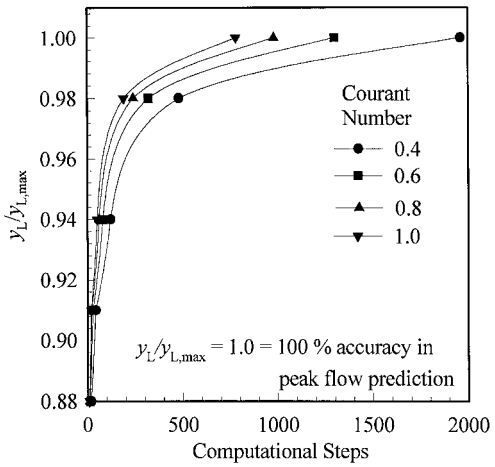

FIG. 2. Effect of Spatial and Temporal Step Size on Computational Efficiency and Numerical Accuracy

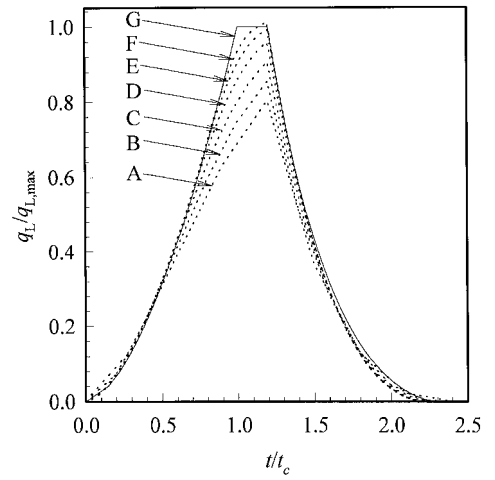

FIG. 3. Sensitivity of Runge-Kutta Modeling Approach to Spatial and Temporal Step Size

J. Hydrol. Eng. 1999.4:165-173.

(G) of the kinematic wave equation. The time of occurrence t is also nondimensionalized by dividing by the time of concentration t_c = 50 min. As Fig. 3 illustrates, the numerical solution approaches that of the MOC analytical solution as the number of spatial and temporal steps are increased. Determining the point at which further increases in N_{space} and N_{time} only marginally improve the numerical results is subjective but is based on both the input data uncertainty and the desired level of accuracy. For this example, E with (20, 39) provides a satisfactory estimate of the peak using approximately four times fewer computational steps than F with (40, 79). Next, the fourth-order Runge-Kutta modeling approach is compared with a higher-order finite-element model.

COMPARISON TO HIGHER-ORDER NUMERICAL METHODS

The numerical accuracy of the Runge-Kutta finite-difference (RK4 FD) modeling approach is compared with a more complex finite-element method using the results of a hypothetical watershed simulation, first presented by Muñoz-Carpena et al. (1993). A hillslope 15 m in length, with a Manning's roughness coefficient of 0.048 and a slope of 5.76%, experiences a rainfall of 3.33×10^{-6} m/s for a duration sufficient to achieve steady flow over the catchment.

Figs. 4 and 5 show the results of the Petrov-Galerkin finite-element (PG FE) modeling approach as presented by Muñoz-Carpena et al. (1993), an MOC analytical solution, and the RK4 FD modeling approach. In accordance with the finite-element solution, the finite-difference solution is computed with a spatial step size of 0.3 m and a temporal step size of 3.6 s. The Courant number is 1.0 for peak flow conditions. In Fig. 4, the MOC analytical solution and the PG FE modeling approach appear as one solid line, due to the scale of the plot. As expected, the finite-difference method slightly smoothes the

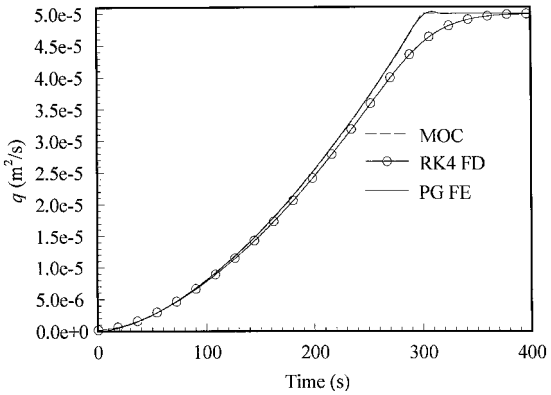

FIG. 4. Comparison of Runge-Kutta, Petrov-Galerkin, and MOC Modeling Approaches

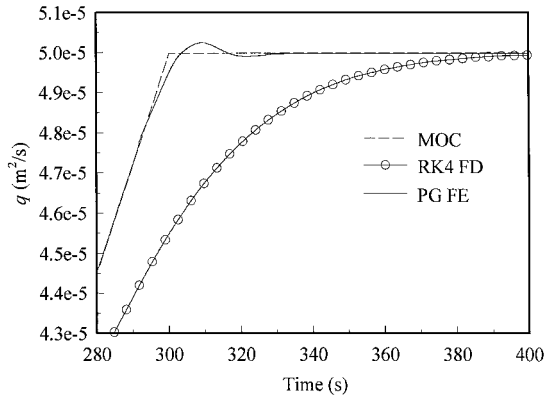

FIG. 5. Comparison of the Runge-Kutta, Petrov-Galerkin, and MOC Modeling Approaches at Peak Runoff

response due to the presence of numerical diffusion. Further refinement of the spatial and temporal grid will reduce the numerical diffusion evident in Fig. 5, and result in less attenuation of the peak. However, roots, soil deposits on the bedrock face, and changes in topography introduce diffusion-like effects to the response of a natural watershed. Therefore, some numerical diffusion may partially compensate for neglected natural physical diffusion. If the amount of diffusion is expected to be negligible, it would be necessary to obtain a more accurate solution of the kinematic wave equations (e.g., MOC analytical solution).

Clearly, the RK4 FD modeling approach is a good overall approximation of both the PG FE modeling approach and the MOC analytical solution. Moreover, the PG FE modeling approach is more computationally expensive than the RK4 FD approach. Although testing the numerical accuracy of a hydrologic model is an important and necessary step, application to a gauged watershed is a stronger test of its capability.

MODEL APPLICATION

The RK 4 FD modeling approach is applied to a forested watershed near Dorset in Ontario, Canada. Located in the Canadian Shield, this watershed comprises a sandy basal till soil overlying a relatively impermeable granite bedrock. Since the physical and hydrologic characteristics of the watershed are described in detail by Peters et al. (1995), only the most important details are presented here.

The Julian Day (JD) 272 front rainfall and corresponding runoff event are used to test the applicability of the RK4 FD modeling approach to forested watersheds. Details of this rainfall-runoff event are found in Peters (1994). Although evapotranspiration data for this storm event is not available, a value of 5 mm/day is reasonable for prevailing conditions. The soil cover ranges from 0 to 1.5 m, and both the vertical and horizontal hydraulic conductivities are high (0.072−0.72 m/h). As a result, overland flow does not contribute to total runoff production except during very high intensity precipitation events or in areas conducive to exfiltration. The combined effect of these characteristics is a rapidly responding watershed.

Two representative sites (see Peters et al. 1995) within the watershed were monitored for combined surface and subsurface runoff. A trench installed at the most downstream limit of each site collected runoff from the soil surface layer, bedrock face, and an intermediate soil layer. Each site consisted of one deep-soil catchment (namely, catchments contributing to trench 1A and trench 2A) and one shallow-soil catchment (namely, catchments contributing to trench 1B and trench 2B). In this paper, the catchment contributing to trench 2B (herein referred to as catchment 2B) is used to calibrate the RK4 FD modeling approach and catchment 2A (contributing to trench

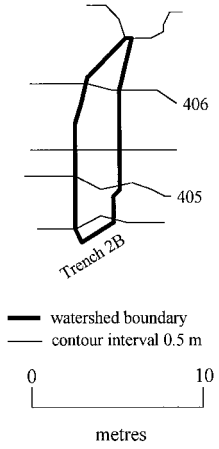

FIG. 6. Bedrock Topography of Catchment 2B

J. Hydrol. Eng. 1999.4:165-173.

2A) is used as a preliminary verification of the RK4 FD modeling approach. The general locations of trenches 2B and 2A are indicated in Figs. 6 and 10.

Parameter Estimation and Calibration

Catchment 2B is a small 23 m^2 microcatchment adjacent to the larger catchment 2A. The bedrock topography of catchment 2B is shown in Fig. 6. As shown in Fig. 7, catchment 2B is modeled as three subcatchments (computational steps). The physical dimensions of each subcatchment (i.e., $W_c \times L_c$) are as follows: Subcatchment 1 is 1.54 m × 2.22 m, while subcatchments 2 and 3 are both 2.22 m × 4.41 m. The largest spatial step size in the catchment is 4.41 m, and a time step of 0.06 hr is adopted to avoid numerical instability. Parameters describing the hydrologic and physical characteristics of catchment 2B are summarized in Table 1. Each parameter is from the work of Peters et al. (1995), estimated from the soil analysis of Peters (1994), or chosen from the guidelines published in the Ministry of Transportation of Ontario Drainage Manual (1983). Due to the availability of soil suction head from pressure plate tests (Peters 1994) and vertical hydraulic conductivity data, the Green-Ampt infiltration model is employed. As noted, the high vertical hydraulic conductivity of the soil in this watershed effectively excludes the possibility of overland flow. Therefore, selection of the optimal set of parameters—one that provides the best match between observed and computed runoff hydrographs—concentrates on the calibration of subsurface parameters. The horizontal hydraulic conductivity of the soil is deemed the most uncertain of the estimated parameters. In a private communication to the authors, J. M. Buttle suggested that, based on new infiltrometer measurements, K_h may be about one order of magnitude greater than the measurements reported in Peters et al. (1995). Therefore, the initial calibration concentrated on K_h.

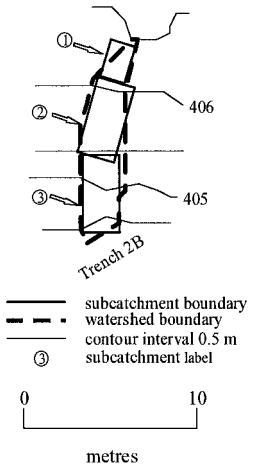

FIG. 7. Subcatchment Dimensions for Prototype Model of Catchment 2B

TABLE 1. Hydrologic and Physical Characteristics of Catchments 2A and 2B

Parameter (1)	Value for 2A (2)	Value for 2B (3)
(*a*) Surface		
Manning's coefficient, n	0.05	0.05
Depression storage depth, D_p	10 mm	10 mm
Average slope, S	18%	15%
(*b*) Subsurface		
Average slope, S_g	18%	15%
Average depth of soil cover, H_t	0.31 m	0.14 m
Soil water content, ω	20%	20%
% of ω for retention storage, ω_r	1%	1%
Soil porosity, ε	70%	70%
Horizontal hydraulic conductivity, K_h	0.72 m/h	0.72 m/h
Vertical hydraulic conductivity, K_v	0.72 m/h	0.72 m/h
Soil suction head, ψ	0.05 m	0.05 m

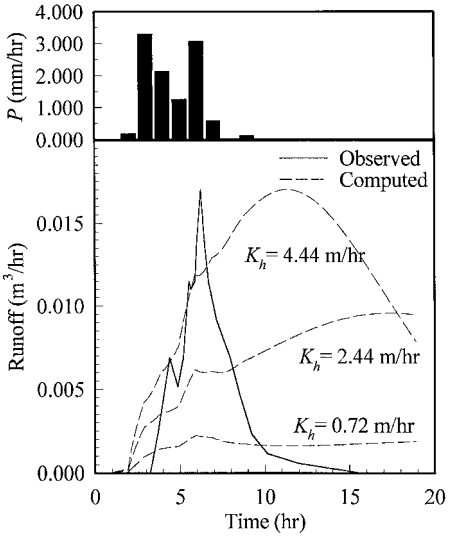

FIG. 8. Calibration Using Darcy's Law

Preliminary Evaluation

As Fig. 8 illustrates, calibration of the RK4 FD modeling approach was unsuccessful. When compared with the observed hydrograph, the computed hydrograph underpredicts the peak runoff and overpredicts the time-to-peak for K_h = 0.72 m/h and K_h = 2.44 m/h. Although computed results for K_h = 4.44 m/h show a marked improvement in the estimation of peak runoff, the peak itself is still significantly delayed. There is also a large mass balance error between the observed and computed runoff hydrographs. The observed hydrograph represents only 20% of the JD 272 rainfall event. The computed hydrographs account for 100% of the JD 272 rainfall event. In effect, the observed hydrograph shows that 80% of the rainfall event is stored in the subsurface of catchment 2B and the 20% that runs off does so at a significantly higher rate than predicted by Darcy's Law. These results indicate that subsurface runoff from a forested shallow-soil watershed is poorly represented as a Darcian process. This conclusion is consistent with Peters et al. (1995), who observed a 0.01-m-thick channel layer between the soil mass and the bedrock face through which it was believed most of the subsurface flow was conducted. Thus, an alternative subsurface model was sought.

Extended Subsurface Model

In the modified representation, the subsurface is divided into two storage components—a rapidly responding macropore store and a slower responding micropore store. In effect, continuous subsurface flow is partitioned into two discontinuous flow paths (i.e., flow as a result of changing macropore storage and flow as a result of changing micropore storage). This conceptual model of the overall continuous soil media has been used previously by Ormsbee and Kahn (1989) to predict subsurface runoff from steeply sloping watersheds. The RK4 FD modeling approach differs from Ormsbee and Kahn (1989) in that a partition of infiltration, not precipitation, delineates each store. In addition, runoff from the macropore store is modeled as a continuous channel using Manning's equation. Clearly this is a conceptual description, despite the use of physically based equations.

The mass-balance equation governing the rate of change of micropore water depth f_{mi} for the subcatchment micropore store is

J. Hydrol. Eng. 1999.4:165-173.

$$f_{\text{mi}}[t, H(t)]_j = \frac{d(H_r + H_i)_j}{dt} = \frac{(1 - \alpha) f_i + g_{j-1} - g_j - E}{\varepsilon} \quad (12)$$

in which $H = (H_r + H_i)_j$ = total depth of water in micropore store within subcatchment j; H_i = drainable depth of water in micropore store; α = fraction of infiltration entering macropore store; g_{j-1} = subsurface runoff from subcatchment $j - 1$ micropore store directly upstream of subcatchment j; and g_j = subsurface runoff from subcatchment j micropore store. Runoff from the micropore store is calculated by Darcy's Law

$$g = K_i \frac{H_i}{L_c} S_g \quad (13)$$

in which K_i = horizontal conductivity of micropore store.

The mass-balance equation governing the rate of change of macropore water depth f_{ma} for the subcatchment macropore store is

$$f_{\text{ma}}[t, M(t)]_j = \frac{d(M_p + M_a)_j}{dt} = \alpha f_i + m_{j-1} - m_j \quad (14)$$

in which $M = (M_p + M_a)_j$ = total depth of water in macropore store within subcatchment j; M_a = drainable depth of water in macropore store; m_{j-1} = subsurface runoff from subcatchment $j - 1$ macropore store directly upstream of subcatchment j; m_j = subsurface runoff from subcatchment j macropore store; and M_p = subsurface depression storage representing average depth of water trapped by plant roots and soil deposits strewn across bedrock face. The existence of a channel between the soil layer and the bedrock face suggests that flow over the bedrock face is more akin to overland flow than porous media subsurface flow. Given this observation, Manning's equation is proposed as an alternative approach to modeling subsurface flow in catchment 2B. In symbols

$$m = \frac{C_u}{n_s L_c} M_a^{5/3} S_g^{1/2} \quad (15)$$

in which n_s = Manning's roughness coefficient for subsurface channel, a parameter deserving special attention.

On examination of the subsurface channel cross section, it is clear that the wetted perimeter of the flow path is substantially larger than the watershed width (i.e., $W_c + 2H_d$) assumed in (15). In effect, the presence of a complex network of plant roots reduces the cross-sectional area of the flow path and significantly increases its wetted perimeter. To quantify these effects, n_s is used as a scale factor for hydraulic losses in catchment 2B. As a result, large subsurface Manning's coefficients, probably greater than 1.0, are anticipated.

Calibration Using Extended Subsurface Model

Calibration of the RK4 FD modeling approach using the extended subsurface model concentrates on obtaining the optimal combination of α, M_p, and n_s. The horizontal conductivity of the micropore store K_i is assumed to equal K_h = 0.72 m/h, and the retention storage ω_r = 1%. Both are obtained from Table 1, and $H_r = \omega_r(\omega H_d)$ as earlier. The value of α is approximated by dividing the total runoff using the rainfall-runoff data from Peters (1994). For numerous combinations of M_p and n_s, the computed runoff hydrograph is compared with the observed hydrograph until the best match is obtained. The optimal set of subsurface calibration parameters for catchment 2B are α = 0.2, n_s = 1.2, and M_p = 0.4 mm.

Evaluation of Extended Subsurface Model

Calibration of the RK4 FD modeling approach using the extended subsurface model is more successful than the dedicated Darcian flow calibration. During the storm event, the micropore store contribution to total subsurface runoff is between 0.15 and 100%. At the peak, the micropore store contributes 0.28% of the total subsurface runoff. However, by t = 11 h this contribution rises to 10%, and by t = 17 h the micropore store is contributing fully 50% of the total subsurface runoff. As Fig. 9 shows, the computed hydrograph underpredicts the observed hydrograph by only 0.0005 m^3/h and overpredicts the time-to-peak by approximately 15 min. In addition, there is a negligible mass balance error between the observed and computed hydrographs. This is a decided improvement over the previous calibration study. However, the secondary peak, occurring at 4.5 h in both the observed and computed hydrographs, differs by 0.0055 m^3/h. Since this catchment is small and approximately 50 m from the rain gauge (see Fig. 10), spatial variability of rainfall may account for this discrepancy. That is, the measured rainfall during the first three or four hours of the storm event is unlikely to accurately represent the rainfall on the catchment, a common problem when modeling small watersheds. Given that discrepancies between the computed and observed hydrographs can be rationalized, the calibration procedure is considered satisfactory. In the next section, the RK4 FD modeling approach is applied to the nearby and much larger catchment 2A.

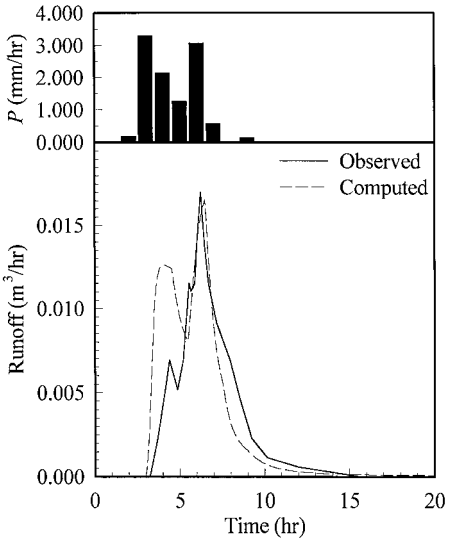

FIG. 9. Calibration Using Extended Subsurface Model

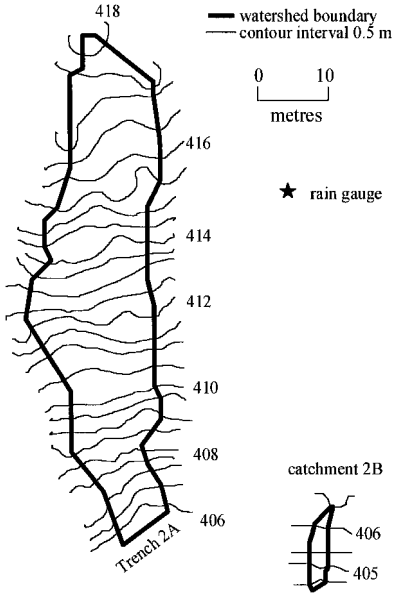

FIG. 10. Bedrock Topography of Catchment 2A

J. Hydrol. Eng. 1999.4:165-173.

Verification

Catchment 2A has a drainage area of 822 m^2 and is described by the hydrologic parameters of Table 1 and the bedrock topography of Fig. 10. Catchment 2A is adjacent to catchment 2B and as such it shares many of the same hydrologic parameters. For example, the horizontal conductivity of the micropore store K_i is assumed to equal K_h = 0.72 m/h, and the percentage of ω for retention storage ω_r = 1%. Both are obtained from Table 1, and $H_r = \omega_r(\omega H_d)$ as earlier. The optimal set of subsurface calibration parameters from catchment 2B (i.e., n_s = 1.2 and M_p = 0.4 mm) are directly employed in the computation of the runoff hydrograph for catchment 2A. Once again, the value of α is estimated from the storm event data of Peters (1994). For catchment 2A, α = 0.13. Characterization of macropore flow as a single subsurface channel has not been previously tested in the literature. In addition, a methodology has yet to be developed to obtain initial estimates of the calibration parameters for other watersheds. Therefore, the physical representation of these parameters should be considered provisional until further testing is complete.

As Fig. 11 shows, catchment 2A is modeled as eight subcatchments. The physical dimensions of each subcatchment are listed in Table 2. To reduce the effects of numerical diffusion, each subcatchment is further subdivided into six identical subcatchments (spatial steps) with one upslope of the other. Thus, the largest spatial step size in the catchment is 1.92 m, which is comparable to that employed in the calibration procedure. A time step of 0.06 h is chosen to ensure numerical stability. Using a 100 Mhz Pentium processor, execution times are less than 15 s for both catchment 2A and 2B.

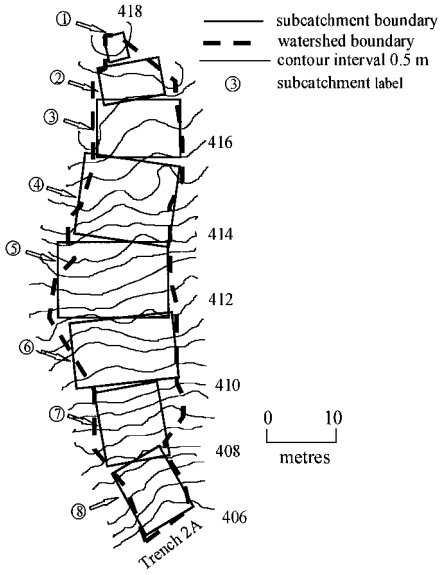

FIG. 11. Subcatchment Dimensions for Prototype Model of Catchment 2A

TABLE 2. Subcatchment Dimensions for Prototype Model of Catchment 2A

Subcatchment (1)	W_c (m) (2)	L_c (m) (3)
1	3.19	3.83
2	9.14	5.53
3	12.34	8.30
4	13.93	11.49
5	16.23	10.85
6	14.98	9.36
7	9.36	10.64
8	8.09	10.00

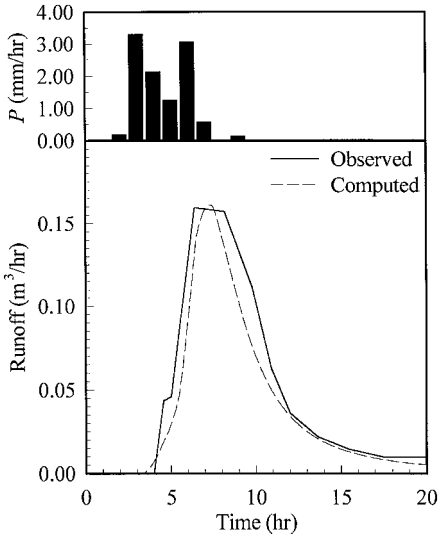

FIG. 12. Verification Using Extended Subsurface Model

Comparison of the computed and observed runoff hydrographs in Fig. 12 shows that the time-to-peak, peak runoff, and total runoff volume are satisfactorily predicted by the model. During the storm event, the micropore store contribution to total subsurface runoff is between 0.14 and 100%. At the peak, the micropore store contributes 0.15% of the total subsurface runoff. By t = 20 h this contribution rises to 3%. Given the encouraging results of this preliminary analysis, the RK4 FD modeling approach shows promise. Clearly, one storm event and one catchment is insufficient to validate the RK4 FD modeling approach. However, the intent of this paper is to show that simple storage concepts can be used by practicing engineers to quickly and easily approximate runoff from a forested shallow-soil watershed. This simplified approach has important advantages. One of the major virtues of the RK4 FD modeling approach is the ease with which physical and hydrologic characteristics are selected, changed, and their effect displayed. The resulting hydrograph from each subcatchment is automatically stored to enable comparison with existing rainfall-runoff data. The user can then interpret the sensitivity of the modeling procedure to different physical assumptions. To avoid overemphasizing the level of detail in describing catchment characteristics, the RK4 FD modeling approach permits the user to develop a prototype sequentially. That is, the user starts with a crude representation of the watershed and then progressively refines the prototype as necessary. By analyzing the predicted response to each refinement, the user develops better judgment for the appropriate level of discretization required. Thus the model encourages the user to adopt a ''top down'' approach, one that resolves the major hydrologic issues, before proceeding with a detailed analysis of the physical and hydrologic parameters of the watershed.

CONCLUSIONS

A spatially lumped hydrologic model is mated to a fourth-order Runge-Kutta ordinary differential equation solver. Results of this study show that a Runge-Kutta solution allows a rapid and efficient integration of the conservation of mass and runoff equations. The Runge-Kutta modeling approach is a more stable solution of the surface-subsurface flow approximation than the conventional Euler approach used in many commercial models. The greater stability of the Runge-Kutta method permits the use of a finer spatial step, which results in a more accurate computed response.

Comparison with higher-order models shows that the Runge-Kutta approach can approximate the MOC analytical solution almost as well as a much more complex finite-element

solution. Less computational expense and the more than adequate ability to approximate the MOC analytical solution of the kinematic wave equations makes the Runge-Kutta approach an attractive alternative to complex numerical solutions for many practical watershed modeling applications.

Initial testing of the model on a forested shallow-soil watershed yielded poor results, probably because Darcy's Law poorly represents the rapid response of the watershed via small channels along the soil-bedrock interface. An extended subsurface model is proposed in which the subsurface runoff process is represented by both Darcy's Law and Manning's Equation. A preliminary analysis of the extended model shows good agreement with observed runoff hydrographs for the same watershed. Although more research is needed to comprehensively validate the model, the Runge-Kutta approach satisfactorily predicts both the peak runoff and the total volume of runoff from the study watershed for one event.

Hydrologically, the Runge-Kutta approach is simple and direct, but from the user's point of view it is flexible, interactive, and avoids some calibration parameters, such as the time of concentration. For this reason, the emphasis in the Runge-Kutta approach is on developing a sense of how natural water transport and storage mechanisms attenuate and delay the effects of runoff conditions. Only once the user develops this feeling for the response of a watershed can a degree of stability and predictability be realized in the model output.

ACKNOWLEDGMENTS

The writers wish to thank the Natural Sciences and Engineering Research Council of Canada for financial support.

APPENDIX I. REFERENCES

Axworthy, D. H. (1993). "A numerical kinematic model for surface and subsurface hydrologic processes," Master's thesis, University of Toronto, Toronto.

Beven, K. (1981). "Kinematic subsurface stormflow." *Water Resour. Res.*, 17(5), 1419–1424.

Chow, V. T., Maidment, D. R., and Mays, L. W. (1988). *Applied hydrology*. McGraw-Hill, New York.

Engman, E. T., and Rogowski, A. S. (1974). "A partial area model for storm flow synthesis." *Water Resour. Res.*, 10(3), 464–472.

Green, W. H., and Ampt, G. A. (1911). "Studies on soil physics." *J. Agric. Sci.*, 4(Part 1), 1–24.

Holtan, H. N. (1961). "A concept for infiltration estimates in watershed engineering." *Agric. Res. Ser.*, U.S. Dept. of Agriculture, Washington, D.C., 41–51.

Horton, R. E. (1933). "The role of infiltration in the hydrologic cycle." *Trans., Am. Geophys. Union*, 14, 446–460.

Huggins, L. F., and Monke, E. J. (1968). "A mathematical model for simulating the hydrologic response of a watershed." *Water Resour. Res.*, 4(3), 529–539.

James, W. P., and Kim, K. W. (1990). "A distributed dynamic watershed model." *Water Resour. Bull.*, 26(4), 587–596.

Jardine, P. M., Wilson, G. V., Luxmoore, R. J., and McCarthy, J. F. (1989). "Transport of inorganic and natural organic tracers through an isolated pedon in a forest watershed." *Soil Sci. Soc. Am. J.*, 53, 317–323.

Jardine, P. M., Wilson, G. V., McCarthy, J. F., Luxmoore, R. J., Taylor, D. L., and Zelansky, L. W. (1990). "Hydrogeochemical processes controlling the transport of dissolved organic carbon through a forested hillslope." *J. Contam. Hydro.*, 6, 3–19.

Julien, P. Y., and Moglen, G. E. (1990). "Similarity and length scale for spatially varied overland flow." *Water Resour. Res.*, 26(8), 1819–1832.

Ministry of Transportation of Ontario. (1983). *Drainage manual*, Toronto.

Muñoz-Carpena, R., Miller, C. T., and Parsons, J. E. (1993). "A quadratic Petrov-Galerkin solution for kinematic wave overland flow." *Water Resour. Res.*, 29(8), 2615–2627.

Ormsbee, L. E., and Kahn, A. Q. (1989). "A parametric model for steeply sloping forested watersheds." *Water Resour. Res.*, 25(9), 2053–2065.

Peters, D. L., Buttle, J. M., Taylor, C. H., and LaZerte, B. D. (1995). "Runoff production in a forested, shallow soil, Canadian Shield basin." *Water Resour. Res.*, 31(5), 1291–1304.

Peters, D. L. (1994). "Subsurface flow processes in forested Canadian Shield hillslopes: Contributions to runoff production," Master's thesis, Trent University, Peterborough, Ont., Canada.

Press, W. H., Flannery, B. P., Teukolsky, S. A., and Vetterling, W. T. (1988). *Numerical recipes in C*. Cambridge University Press, Cambridge, Mass.

Priestley, C. H. B., and Taylor, R. J. (1972). "On the assessment of surface heat flux and evaporation using large-scale parameters." *Monthly Weather Rev.*, 100(2), 81–92.

Singh, V. P. (1988). *Hydrologic systems, volume I, rainfall-runoff modeling*. Prentice-Hall, Englewood Cliffs, N.J.

Sloan, P. G., and Moore, I. D. (1984). "Modeling subsurface stormflow on steeply sloping forested watersheds." *Water Resour. Res.*, 20(12), 1815–1822.

"USDA-water erosion prediction project: User summary." (1995). *NSERL Rep. No. 11*, D. C. Flanagan and S. J. Livingston eds., USDA-ARS National Soil Erosion Research Laboratory, West Lafayette, Ind.

APPENDIX II. NOTATION

The following symbols are used in this paper:

a = catchment scaling factor;
C_r = Courant number;
C_u = constant depending on units;
D = total storage depth;
D_t = detention storage depth;
D_p = depression storage depth;
E = evapotranspiration rate;
f_g = rate of change of subsurface water depth;
f_{ma} = rate of change of macropore water depth;
f_{mi} = rate of change of micropore water depth;
f_s = rate of change of surface water depth;
f_i = infiltration rate;
g = subsurface runoff from subcatchment;
$\mathbf{g}$ = acceleration due to gravity;
g_j = subsurface runoff from subcatchment in question;
g_{j-1} = subsurface runoff from subcatchment directly upstream of subcatchment in question;
H_d = drainable depth of water stored in hillslope saturated zone;
H_i = drainable depth of water in micropore store;
H_r = retention storage;
H_t = depth of soil cover;
K_h = horizontal saturated hydraulic conductivity;
K_i = horizontal conductivity of micropore store;
K_v = vertical saturated hydraulic conductivity;
k_1, k_2, k_3, k_4 = Runge-Kutta method constants;
L_c = dimension of subcatchment parallel to direction of flow;
M_a = drainable depth of water in macropore store;
M_p = subsurface depression storage;
N_{space} = number of spatial step sizes;
N_{time} = number of time steps;
n = Manning's roughness coefficient;
n_s = subsurface Manning's roughness coefficient;
$O(\Delta t^5)$ = error term;
P = base rate of rainfall;
q = overland flow from subcatchment;
q_j = overland flow from subcatchment in question;
q_{j-1} = overland flow from subcatchment directly upstream of subcatchment in question;
q_L = unit surface discharge;
$q_{L,\max}$ = maximum unit surface discharge;
R = hydraulic radius;
S = surface subcatchment slope;
S_g = slope of subsurface bed;
t = time;
t_r = duration of storm event;
W_c = dimension of subcatchment perpendicular to direction of flow;
y_L = surface flow depth;
$y_{L,\max}$ = maximum surface flow depth;

J. Hydrol. Eng. 1999.4:165-173.

y_{pk} = peak depth of overland flow;
dH_a/dx = hydraulic gradient;
α = fraction of infiltration entering macropore store;
Δt = time step size;
Δx = spatial step size;
ε = soil porosity;
ν = kinematic viscosity;
ψ = soil suction head;
ω = subsurface water content; and
ω_r = percent of total porous media storage available for storage of retained water.

Subscripts

j = subcatchment index.

J. Hydrol. Eng. 1999.4:165-173.